

Dynamic and static fluorescence anisotropy in biological microscopy (rFLIM and emFRET)

Thomas M. Jovin*, Diane S. Lidke, Janine N. Post
Department of Molecular Biology, Max Planck Institute for Biophysical Chemistry,
37077 Göttingen, Germany

ABSTRACT

Fluorescence anisotropy, a measure of the polarization state of fluorescence emission, is a sensitive measure of molecular rotational motion and of resonance energy transfer (RET). We report here the formalism and application of dynamic and static fluorescence anisotropy measurements primarily intended for implementation in imaging systems. These include confocal laser scanning microscopes (CLSM) as well as wide-field instruments, in the latter case adapted for anisotropy-based dynamic frequency domain fluorescence lifetime imaging microscopy (FLIM), a method we denote as rFLIM. Anisotropy RET is one of the modalities used for fluorescence RET (FRET) determinations of the association, and proximity of cellular proteins *in vivo*. A requirement is the existence of intrinsic or extrinsic probes exhibiting homotransfer FRET (in our nomenclature, energy migration or emFRET) between like fluorophores. This phenomenon is particularly useful in studies of the activation and processing of transmembrane receptor tyrosine kinases involved in signal transduction and expressed as fusions with Visible Fluorescence Proteins (VFPs).

Keywords: green fluorescent protein, GFP, Venus, fluorescence polarization

1. INTRODUCTION

Alterations in molecular size, shape, or state of association are essential elements of the mechanisms responsible for the regulation of cellular function. For cellular studies, one requires specific signals reporting on the status of particular molecules or molecular superstructures. Because of its inherent sensitivity and specificity, fluorescence microscopy is a (the) method of choice. From a photophysical standpoint, the polarization state of fluorescence signals (or more generally, of luminescence) provides the most sensitive measure of the desired molecular parameters. An optimal measure of polarization is the fluorescence anisotropy, defined for the usual geometric configurations of optical systems in the form

$$r = \frac{\Delta i}{i_{tot}} \quad (1)$$

where $\Delta i = I_{\parallel} - I_{\perp}$ and $i_{tot} = I_{\parallel} + 2 I_{\perp}$. Excitation with plane polarized light is assumed; thus I_{\parallel} and I_{\perp} are the emissions

* tjovin@gwdg.de; phone +49-551-201-1381; fax +49-551-201-1467

components polarized in planes parallel and perpendicular, respectively, to that of excitation. The denominator of r , i_{tot} , represents the total emission, assuming that the generally inaccessible projection along the 3rd orthogonal axis (coinciding with the excitation propagation direction) by symmetry is equal to I_{\perp} ; this condition will not hold in general for oriented samples.

If we assume a delta excitation pulse and a single fluorescence moiety with one distinct excited state lifetime τ , the decay laws applying to $i_{tot}(t)$ and $r(t)$ are given by the following relationships:

$$i_{tot}(t) = \bar{i}_{tot} i(t) \quad i(t) = \tau^{-1} e^{-t/\tau} \quad r(t) = (r_o - r_{\infty}) e^{-t/\phi} + r_{\infty} \quad \bar{r} = \int_0^{\infty} i(t) r(t) dt \rightarrow \frac{r_o - r_{\infty}}{\bar{r} - r_{\infty}} = 1 + \sigma \quad (2)$$

where \bar{i}_{tot} and \bar{r} are steady-state quantities, applicable under conditions of constant illumination; r_o , r_{∞} , ϕ , and σ are the fundamental (initial) anisotropy, the limiting anisotropy (in the event of hindered motion), the rotational correlational time, and the normalized rotational parameter ($\sigma = \tau / \phi$), respectively. Most of the anisotropy formalism is based on dimensionless ratios of intensities and time constants. Thus, the corresponding equations and measurements are relatively insensitive to parameters such as optical light path and absolute intensity, implying that anisotropy should be well suited for implementation in cellular microscopy.

Fluorescence depolarization reflects the degree to which the molecular frame of the fluorophore rotates during the excited state lifetime, leading to a loss of correlation between the relative spatial orientation of the absorption and emission transition dipoles from that characteristic of the immobile molecule. Molecules with arbitrary shape exhibit a complex anisotropy decay law with numerous correlation times. However, in most (practical) situations applicable to the microscopy of cells, molecular asymmetry and/or the influence of an anisotropic microenvironment, such as a lipid bilayer, can be accounted for adequately by the relationship of Equation 2. That is, most degrees of structural complexity can be accommodated by apparent values of r_{∞} and ϕ . The latter parameter is very sensitive to the formation of molecular complexes such as in self or hetero-association or integration into a supramolecular structure, inasmuch as the correlation time is proportional to molecular volume and the operational microviscosity. (By way of orientation, for a globular protein in aqueous solution, $\phi \approx 0.6$ ns/kDa.)

One of the most sensitive techniques for measuring time dependent fluorescent anisotropy is based on the detection of the relative phase and modulation of the two polarized emission components in a frequency domain instrument. We have reported¹⁻³ the adaptation of the concepts and experimental realization pioneered by Gregorio Weber and coworkers to a wide-field microscope and denoted the technique as anisotropy (r) fluorescence lifetime imaging microscopy (rFLIM).

The anisotropy also decays in response to fluorescence resonance energy transfer (FRET). This process involves the transfer of energy from a photoselectively excited donor molecule to a nearby acceptor. In a molecular ensemble undergoing many photophysical cycles, the donor fluorescence exhibits a *hyperpolarization* (relative to the unperturbed state) due to the shortening of its excited state lifetime. In contrast, the emission of the mean acceptor population will be largely depolarized, assuming for the moment the absence of a specific and unique donor-acceptor stereochemical relationship. The donor and acceptor can be distinct entities, engaging in *heterotransfer*, but under some conditions FRET occurs between identical fluorophores, in a process denoted as *homotransfer* or energy migration RET. The magnitude of this effect can be arbitrary, e.g. leading to complete depolarization, and can be quantified by rFLIM and related microscope systems⁴⁻⁹ as well as by simple steady-state anisotropy determinations in scanning or widefield microscopes^{3, 10, 11}. We have exploited this phenomenon, to which we refer as emFRET (energy migration FRET)¹⁻³, in studies of transmembrane proteins fused to members of the family of visible fluorescence proteins (VFPs). A particular target of our VFP-related research has been the receptor tyrosine kinases of the erbB/HER family mediating cellular

growth and other processes, a principle goal being the determination of the state of association prior to and in response to peptidic growth factors.

2. FORMALISM OF emFRET

2.1 emFRET

An instructive tabulation of the comparative merits of conventional heterotransfer FRET and emFRET is given in Table I. The distinctive feature of emFRET occurring between an ensemble of molecules is that its only manifestation is depolarization, i.e. a decrease in anisotropy, with no change in the lifetime or spectral properties, as opposed to the characteristic donor quenching and sensitized acceptor emission observed in heterotransfer FRET.

Table I. Heterotransfer vs. homotransfer(em) FRET

<i>Properties of the molecular ensemble</i>	<i>heterotransfer</i>	<i>homotransfer(em)</i>
need distinct donor-acceptor pair	+	-
donor quenching	+	-
donor lifetime	↓	n.c.
donor anisotropy	↑	↓
acceptor anisotropy	↓	n.a.
optimal donor Stokes shift	large	small
donor "spreading"	-	+
acceptor sensitization	+	n.a.
no. of transfers	1 (trap)	≥1
orientational dependence	+	-
rFLIM assay	+	+

n.c., no change; n.a., not applicable

In the event that both rotational diffusion and emFRET are operative during the excited state lifetime, the formalism for $r(t)$ and \bar{r} is considerably more complex. Fortunately, the particular properties of the VFPs allow for significant simplification in that the terms accounting for the two processes can be combined as a product². The rotational diffusion of the 27 Kda monomeric VFPs is limited during their relatively short fluorescence lifetime of 1-3 ns compared to the ~18 ns rotational correlation time, ϕ^{12} ; thus $\sigma = 0.06-0.17$. Under these circumstances, the concentration depolarization due to emFRET is given by

$$\bar{r} = \bar{r}_o(1 - dp[\beta]) \quad dp[\beta] = \beta e^{\beta^2} \pi^{1/2} erf(\beta) \quad (3)$$

where \bar{r}_o is the steady-state anisotropy in the absence of emFRET and is given by Equation 2 with $r_\infty = 0$; erf is the error function. The parameter β incorporates the concentration dependence of emFRET.

$$\beta = \frac{\alpha c}{2\sqrt{1 + \sigma}} \quad \alpha \approx R_o^3 / 375; \text{ units, nm}^3 \text{ (see ref. } ^2) \quad (4)$$

R_o is the Förster transfer distance defined for a single donor-acceptor pair exhibiting the 6th power law for the transfer efficiency E and c is the concentration in mM units.

$$E = [1 + (r/R_o)^6]^{-1} \quad R_o = 8.79 \cdot 10^{-28} J n^{-4} \kappa^2 Q \text{ (see ref. } ^{13}) \quad (5)$$

where r is the distance between donor and acceptor, J is the spectral overlap integral (a measure of donor emission and acceptor absorption overlap), n is the refractive index of the medium between donor and acceptor, κ^2 is the orientation factor (a measure of the relative transition moment orientation), and Q is the unperturbed donor fluorescence quantum yield (but see ref. ¹⁴).

2.2 rFLIM

The theory of differential phase fluorimetry and the implementation of the technique in a full-field microscope has been described in detail elsewhere². It suffices to state at this juncture that the measurements require determinations of the phase shifts and demodulation of the two polarized emission components, using an intensity-modulated light source instead of the delta forcing function assumed in Equation 2. The measured quantities are derived from comparisons between the two signals as a function of excitation radial frequency ω : the differential phase $\Delta\Phi$, the AC modulation ratio Y_{AC} , and the DC ratio Y_{DC} . The rotational diffusion parameters (r_o, r_∞, ϕ) are analytical functions of $\Delta\Phi$, Y_{AC} , and Y_{DC} ².

The analytical expressions for $\Delta\Phi$ and Y_{AC} incorporating emFRET are given here for the first time (Equations 6 and 7); Y_{DC} is directly related to \bar{r} via Equations 3 and 8. The only additional parameters are α (Equation 4) and the concentration c . The effect of emFRET on the rFLIM parameters is to increase $\Delta\Phi$ and decrease Y_{AC} and Y_{DC} in a concentration and frequency dependent manner (Figure 1). However, above certain values of αc (~ 1 with the parameters specified in Figure 1), $\Delta\Phi$ decreases with c and ω . The effect of finite measurement noise in the simulation of Figure 1 has been represented as dot plots bound by the ± 2 s.d. limits of the distributions. In interpreting these results, one should consider that in an imaging context, regions of interest usually comprise numerous pixels, such that an adequate precision can be achieved. The parameters $\Delta\Phi$ and Y_{AC} , as well as the functions for the individual polarized emission signals $I_{||}$ and I_{\perp} (not shown), also depend strongly on the modulation frequency (Figure 2 in ref.³).

$$\Delta\Phi = \tan^{-1} \left[\frac{3r_o(f_c + f_s\gamma)}{1 - r_o[f_c(\gamma + 2f_c r_o(1 + \gamma^2)) - f_s(1 - 2f_s r_o(1 + \gamma^2))]} \right] \quad (6)$$

$$Y_{AC} = \sqrt{\frac{[2r_o(1 + \gamma^2)f_c - \gamma]^2 + [1 + 2r_o(1 + \gamma^2)f_s]^2}{[r_o(1 + \gamma^2)f_c + \gamma]^2 + [1 - r_o(1 + \gamma^2)f_s]^2}} \quad (7)$$

$$Y_{DC} = \frac{1 + 2\bar{r}}{1 - \bar{r}} \quad (8)$$

where,

$$\gamma = \omega\tau; f_1 = \frac{\alpha c}{2\sqrt{(1 + \sigma) - i\gamma}}; f_2 = \text{Re}[erfc(f_1)]; f_3 = \text{Im}[erfc(f_1)]; f_4 = \sqrt{(1 + \sigma)^2 + \gamma^2}$$

$$f_5 = \sqrt{f_4 - (1 + \sigma)}; f_6 = \sqrt{f_4 + (1 + \sigma)}; f_7 = [f_2(1 + \sigma) - f_3\gamma]; f_8 = [f_3(1 + \sigma) - f_2\gamma]; f_9 = \frac{\alpha c^2 \gamma}{4f_4^2}$$

$$f_c = \frac{1}{f_4^2} \left[\frac{\alpha c e^{\frac{\alpha c^2(1 + \sigma)}{4[\gamma^2 + (1 + \sigma)^2]}} \sqrt{2\pi}}{4f_4} [(f_5 f_7 + f_6 f_8) \cos(f_9) + (f_6 f_7 - f_5 f_8) \sin(f_9)] - \gamma \right]$$

$$f_s = \frac{1}{f_4^2} \left[\frac{\alpha c e^{\frac{\alpha c^2(1+\sigma)}{4[\gamma^2+(1+\sigma)^2]}} \sqrt{2\pi}}{4f_4} [(f_5 f_8 + f_6 f_7) \cos(f_9) + (f_6 f_8 - f_5 f_7) \sin(f_9)] + (1+\sigma) \right]$$

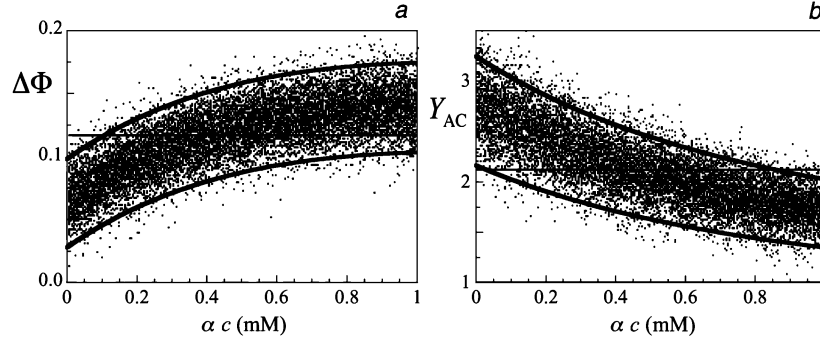


Figure 1. Combined rFLIM and emFRET. Simulation of the concentration dependence of $\Delta\Phi$ (a) and Y_{AC} (b) in the presence of Gaussian experimental noise. Parameters corresponding to a typical VFP: τ , 3 ns; ϕ , 19 ns; r_o , 0.39; s.d. $\Delta\Phi$, $\pi/180$; s.d. Y_{AC} , 0.1. Solid lines, ± 2 s.d. limits. Concentration range αc , 0-1 (for $R_o = 5$ nm, $\alpha = 0.33$, corresponding to a maximal concentration c of 3 mM). Modulation frequency f , 58 MHz ($\omega = 2\pi f$).

2.3 emFRET in a dilute monomer-dimer equilibrium

Equation 3 applies to a 3-dimensional solution, i.e. a statistical ensemble of randomly oriented molecules with a distribution of separation distances determined by the bulk concentration. However, in the event that molecules form distinct complexes, such as a dimer, the orientation between the two constituting monomers will in general be unique and thus dictate the extent of intramolecular transfer depolarization. As a consequence, two distinct emitting species can be envisioned, a monomer (m) and a dimer (d), present at fractional molecular concentrations (relative to the total monomer concentration and dictated by the mass action equilibrium relationship), v_m and $(1 - v_m)/2$, respectively. Each species will possess a distinctive set of rotational diffusion parameters (r_o , r_∞ , ϕ) and thus of \bar{r} ; in the following discussion of fairly globular proteins in free solution, we consider $r_\infty = 0$. We assume that the equilibration of activation energy between the two monomers constituting d is achieved during the excited state lifetime, a condition that is satisfied if the transfer rates in both directions, k_t and k_{-t} , are $\gg \tau^{-1}$, leading to a transfer fraction $\delta = k_t / (k_t + k_{-t})$. From the additivity law of anisotropy, the steady-state anisotropy of the total population, $\langle \bar{r} \rangle_d$, is given by

$$\begin{aligned} \langle \bar{r} \rangle_d &= v_m \bar{r}_m + (1 - v_m) \bar{r}_d \approx [\psi + v_m(1 - \psi)] \bar{r}_m & v_m &= \varepsilon(\sqrt{1 + 2/\varepsilon} - 1) & \varepsilon &= \frac{K_d}{4c} \\ \psi &= \frac{\bar{r}_d}{\bar{r}_m} = \frac{2(1 + \sigma)[1 - \delta(1 - \delta\rho)]}{(2 + \sigma)} & \psi_{\delta=1/2} &= \frac{(1 + \sigma)(2 + \rho)}{2(2 + \sigma)} & \rho &= \frac{r_{o,d}}{r_{o,m}} \end{aligned} \quad (9)$$

where v_m is the fraction of monomer units in m , \bar{r}_m and \bar{r}_d are the steady-state anisotropies of m and d , respectively, K_d is the dimer dissociation constant, c is the total monomer concentration, and $r_{o,d}$ is the operative r_o for a dimer subject to intramolecular transfer depolarization by virtue of absorption by one monomer and emission from the other; $r_{o,m}$ refers to the monomer. The ratio ρ accounts for the arbitrarily (and different) relationship between the transition moments for absorption (of a given monomer in d serving as the donor) and for emission (of the second monomer in d

serving as the acceptor) compared to the configuration of the isolated monomer species in which the absorption and emission transition moments correspond to a single chromophore. Factors of 2 (concentration, absorption cross-section) cancel in the second term of the expression for $\langle \bar{r} \rangle_d$. The expression for ψ (Equation 9) incorporates the additional assumptions that the ϕ of d is twice that of m but that the fluorescence lifetimes are the same.

2.4 emFRET in a concentrated monomer-dimer equilibrium

A second level of emFRET occurs if the monomer and dimer species treated in Section 2.3 are subjected to additional FRET exchanges with neighboring molecules randomly distributed in a crowded, concentrated solution (or densely packed in a two-dimensional structure such as the plasma membrane). Thus, we can envision $m \leftrightarrow m$, $m \leftrightarrow d$, $d \leftrightarrow m$, and $d \leftrightarrow d$ interactions of statistical nature depending on the bulk concentration and the state of the m - d equilibrium. Two out of the four possible transfer processes will predominate under most conditions, e.g. $m \leftrightarrow m$ and $d \leftrightarrow m$ in the lower concentration range and $m \leftrightarrow d$ and $d \leftrightarrow d$ in the higher range. A rigorous treatment of this system is extremely complex¹⁵ but we can greatly simplify the analysis by assuming that the four possible concentration depolarization mechanisms operate independently, thereby leading to four equations for β (Equation 4) corresponding to each combination i, j (where i and $j = m$ or d); secondary transfers between m and d are not considered.

$$\begin{aligned} \beta_{ij} &= \zeta_{ij} c_j & \zeta_{ij} &= \frac{\alpha_j}{2\sqrt{1+\sigma_i}} & c_m &= v_m c & c_d &= (1-v_m)c/2 \\ \zeta_{dm} &\cong \zeta_{mm} & \zeta_{md} &\cong \zeta_{dd} & & \cong 1.5\zeta_{mm} \end{aligned} \quad (10)$$

in which the approximations arise from the use of typical VFP parameters and the assumption stated at the end of Section 2.3.

The combination of Equations 9 and 10 provides an expression for the mean steady-state anisotropy of the entire molecular population subjected to the combined depolarizing effects of dimerization and molecular crowding, $\langle \bar{r} \rangle_{d,mc}$.

$$\frac{\langle \bar{r} \rangle_{d,mc}}{\langle \bar{r} \rangle_d} \cong 1 - dp_m[\beta_m] - dp_d[\beta_d] \quad \beta_m \cong \zeta_{mm} v_m c \quad \beta_d \cong (3/4)\zeta_{mm}(1-v_m)c \quad (11)$$

where dp_m and dp_d are the dp functions (Equation 3) representing the emFRET processes acting via monomer (m) and dimer (d) acceptors, respectively.

Simulations using the above relationships demonstrate the operative range of each phenomenon as a function of the respective molecular parameters (Figure 2). It can be seen that $dp_m > dp_d$ at low concentrations, but the relationship is reversed at higher concentrations, e.g. as the dimer species become increasingly populated. Curve 1 in panel *b* represents the transfer depolarization alone, while curve 5 demonstrates the combined effects of both FRET phenomena on the progress and extent of the depolarization.

3. MONOMERIC AND DIMERIC VENUS VFP

We have employed emFRET in studies on the erbB RTK family, which include EGFR, the prototypical receptor for epidermal growth factor (EGF)³. Numerous fusion proteins of EGFR have been generated from the various VFPs. Major considerations have been the potential influence of the VFPs on the distribution and function of the RTKs and/or whether the former undergo interactions resulting in emFRET signals. Conceivably, complexes formed by VFPs with

inherent tendencies to dimerization could bias the distribution of the attached RTKs such as to activate or otherwise affect the functional state of the system. For this reason, we have extended the determination of the concentration depolarization of eGFP² to other members of the VFP family. In the following discussion, we describe the properties of Venus, a variant of eYFP that is characterized by fast and efficient maturation (due to a F46L mutation) and relative environmental insensitivity¹⁶. We bacterially expressed and purified Venus as well as the variant (mVenus) in which we introduced the A206K mutation to destabilize the interfacial interactions responsible for dimerization of many VFPs¹⁷.

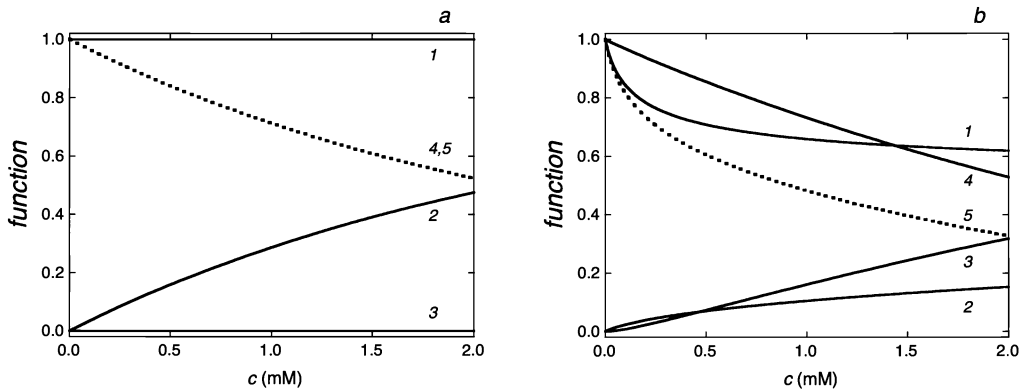


Figure 2. Simulation of emFRET as a function of monomer-dimer equilibrium and molecular crowding. Parameters and functions corresponding to Equations 9-11: (1) $\psi + v_m(1-\psi)$; (2) dp_m ; (3) dp_d ; (4) $1 - dp_m - dp_d$; (5, stippled curve) $[\psi + v_m(1-\psi)][1 - dp_m - dp_d]$. a, depolarization only due to intermolecular transfer between monomers (no dimerization); $\zeta_{mm} = 0.5$, $\psi = 0.2$. b, combined effects of depolarization due to intramolecular and intermolecular transfer; monomer-dimer equilibrium with $K_d = 0.3$ mM.

3.1 Spectral properties of mVenus

The fluorescence excitation, emission and anisotropy spectra of an mVenus solution at low concentration (5 μ M) are shown in Figure 3. The anisotropy was constant over the excitation and emission spectra, with a mean value of 0.324 ± 0.005 and no evidence of the red-edge effect reported for eGFP¹⁰. The overlap integral, J , required for calculation of the Förster emFRET transfer distance R_o was calculated according to procedures in¹³, which yielded the value $2.0 \cdot 10^{32}$ mol⁻¹ nm⁶. The other parameters of R_o were as follows: (i) *refractive index* n . We assumed the value of water (1.33) for intermolecular and of proteins (1.4) for intramolecular transfer; (ii) *orientation factor* κ^2 . For intramolecular transfer, the two chromophores in the crystallographic dimer structure of a GFP mutant (F64L, Y66H)¹⁸ were replaced by the corresponding chromophore of a monomer VFP for which absorption transition moment calculations had been performed¹⁹. The orientation of the vectors in the crystallographic dimer structure corresponding to the deprotonated form of GFP was calculated, as well as two possible positions for the emission transition moment estimated to be at a relative angle ω of $\pm 13 \pm 2^\circ$ (we selected the value 11) using an r_o of 0.37 ± 0.01 for mVenus (Figure 4). The latter value was estimated from the data of Figure 3, Equation 2, σ from Section 2.2, and the expression for the fundamental anisotropy $r_o = 0.2(3\cos^2 \omega - 1)$; the calculated distance between the computed centers of gravity of the two dimer chromophores was 2.4 nm. The resulting value for κ^2 was 3.65 ± 0.05 , reflecting an almost in-line orientation of the respective vectors for absorption and emission. κ^2 for intermolecular transfer was much lower, e.g. 0.476, the value applying to a random but rotationally static distribution of acceptors in an emFRET environment²⁰; (iii) *quantum yield* Q . The literature value of 0.57 was used¹⁶.

Introducing the above values into the expression for R_o , we obtained a value of 6.8 nm for intramolecular emFRET in the VFP dimer and 5.0 nm for intermolecular, emFRET in solution. Using the 6th power law (Equation 5), the forward transfer efficiency in the dimer would be 99.8%. The computed value of $r_{o,d}$ for the emFRET form of the dimer was 0.13 or 0.17, depending on the orientation selected for the emission transition moment.

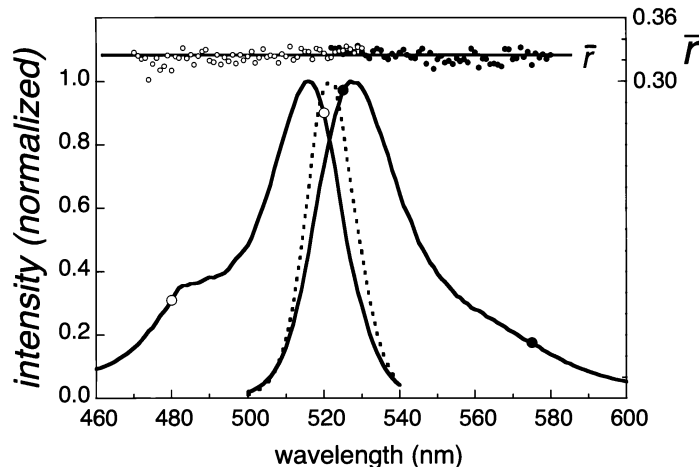


Figure 3. Spectral properties of *mVenus*. Spectra: excitation (○), emission (●), anisotropy excitation (○), and anisotropy emission (●). Conditions: 0.3 μ M protein, 0.1 M Tris-HCl, pH 8.5, 0.1 M NaCl, 20 °C. Excitation spectra with emission measured at 550 nm; emission spectra with excitation at 490 nm. Fluorimeter: Varian Cary Eclipse with motorized polarizers; 100 μ l microcuvettes. The instrumental emission G -factor (optical anisotropy correction) varied in the range 2.1-2.6 from 520-580 nm and was fit to a 2nd-order polynomial before application to the data; a mean G -factor at 550 nm (2.34) was applied to the excitation data. Stippled curve: normalized kernel of the overlap integral for emFRET, J ; the ϵ for Venus was assumed: 92.2 $\text{mM}^{-1} \text{cm}^{-1}$ ¹⁶. The Venus A206K mutation (*mVenus*) was generated using a mutagenesis kit (Stratagene) according to the manufacturer's protocol and with primers as described for eYFP¹⁷.

3.2 Concentration depolarization of *mVenus* and Venus

The parent eYFP of the Venus variants is reported to have a distinct tendency to dimerize, with a reported K_d of 0.11 mM ¹⁷. Thus, in order to utilize Venus with due attention to the potential perturbations on the system under study arising from such VFP-VFP interactions, we investigated the comparative association tendencies of Venus and *mVenus*, as well as other members of the VFP family, using the analytical emFRET tools presented above.

The fluorescence anisotropies of both Venus and *mVenus* decreased with concentration in the range of 0-2 mM (Figure 4). A mayor challenge in such determinations is the prevention of significant self-absorption at the high protein concentrations. This effect was minimized by using a 0.25 mm square cross-section flow cytometer cell (Hellma 131.050-QS) adapted as a microcuvette². The intensities corrected for inner filter effects remained linear, indicative of emFRET as the phenomenon accounting for the concentration depolarization (Figure 4).

The concentration dependence of the fluorescence depolarization of *mVenus* and Venus were very different. Venus demonstrated a steeper and more extensive effect at much lower protein concentration, from which we inferred that it was being subjected to intramolecular emFRET as a consequence of dimerization, in contrast to the A206K mutant (*mVenus*), which is presumed to lack a functional dimerization interface. Thus, the *mVenus* data were fit well with the simple intermolecular emFRET model (case *a* in Figure 4 and Table II), yielding a very plausible r_o value and an R_o for intermolecular emFRET of 5.9 ± 0.1 nm, in reasonably good agreement with the value of 5.0 computed from the spectral

and crystallographic data. The parameters (r_o , R_o) calculated from the fit to the Venus data were physically unrealistic and their precision was low, indicating that Venus is not well described by this model. In contrast, the dimerization model (b) was incompatible with the mVenus curve but yielded plausible values for Venus, e.g. a dimerization K_d of ~ 0.2 mM. The rather large uncertainty in the derived r_o values probably reflected the paucity of points, especially at concentrations $\leq K_d$. As expected, the combined depolarization model (dimerization + molecular crowding, panel c of Figure 4) did not provide better results for mVenus, while the fit to Venus data suffered from the restricted data set (as indicated above) yet yielded reasonable albeit imprecise (with large fit errors) values for r_o , R_o , and ψ . Application of Equation 4 using $\psi = 0.33$ and $r_{o,d} > 0.1$ (Section 3.1) indicated that the fractional emFRET transfer efficiency in the dimeric form of Venus, δ (Equation 9), would have to have exceeded 0.8, implying that back transfer may be unfavorable in this molecule. If so, one can speculate about the existence of transient species arising upon deactivation of the donor excited state^{12, 21} with properties differing from the ground state including a low cross-section for back-transfer from nearby acceptors.

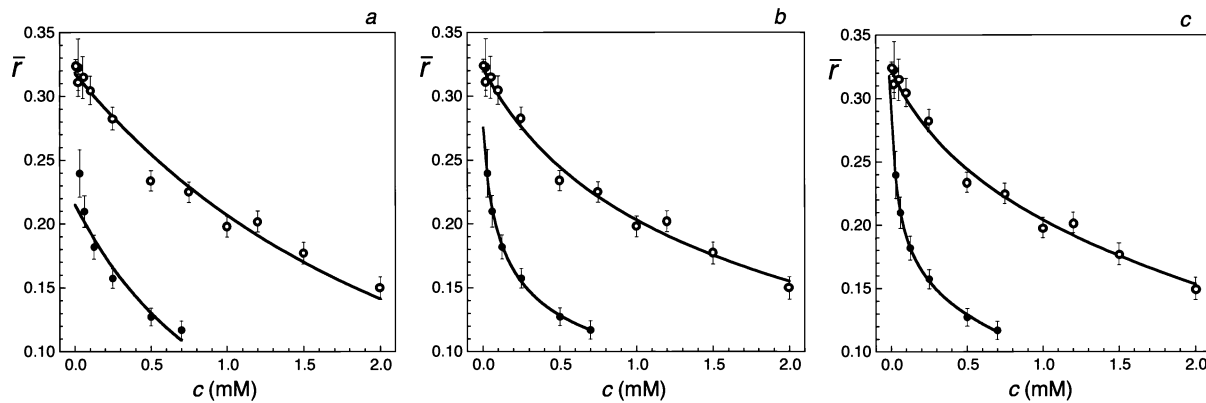


Figure 4. Analysis of concentration depolarization of mVenus (○) and Venus (●). *a*, fit to intermolecular emFRET model (Equation 3). *b*, fit to monomer-dimer equilibrium (Equation 9). *c*, fit to combined monomer-dimer equilibrium (intramolecular emFRET) and intermolecular emFRET involving both monomer and dimer species (Equations 6 and 8). Determinations as in Figure 1; anisotropies, intensity-weighted averages over range 520-580 nm. Fit program: Kaleidagraph 3.6, points weighted by s.d. values (indicated in the plots) estimated from spectral dependence and repeat determinations. The parameters derived from the fits are given in Table II.

4. PERSPECTIVES

The formalism and experimental approach featured in this report are being applied to a number of the VFP family members and this work will be reported elsewhere. These molecules have been fused to various target proteins of interest in signal transduction systems and emFRET is being applied as a means for investigating the underlying molecular interactions in cells. The advantages of emFRET in such studies are many (Table I). We would emphasize in particular the requirement in emFRET for only a single type of probe (fluorophore) such that expression in cells is much simpler than in heterotransfer FRET, for which two different labels must be introduced by transfection or other means and manipulated so to achieve the desired relative stoichiometric levels. For this and other reasons, one can anticipate further implementations of emFRET in a variety of widefield and point scanning microscopes. In addition, fluorescent probes optimized for emFRET, i.e. having (i) a small size, (ii) a large value of r_o , (iii) good photostability, and (iv) a means for

rigid attachment to the target structure (protein, nucleic acid, membrane) are required. Some of these may fall in the category of "indirect" expression probes such as the biarsenylated xanthenes²² and bifunctional rhodamines²³ although these particular compounds may not fulfill all the criteria presented above. Time-resolved studies of the anisotropy decays reflecting the primary transfer process in emFRET, particularly of the VFPs, will further elucidate important details of the underlying transfer mechanism. A very high temporal resolution will be required for these measurements. Finally, the formalism for emFRET must be refined and adapted to the arbitrary and complex two- and three-dimensional distributions characteristic of biomolecules in a cellular context²⁴. Encouraging results have been obtained in studies of lipid microdomains ("rafts") and proteins therein²⁵.

Table II. emFRET analysis of mVenus and Venus according to different formalisms

<i>Fit</i>	<i>Mechanism of concentration depolarization</i>	<i>Parameter</i>	<i>mVenus</i>	<i>Venus</i>
<i>a</i>	intermolecular emFRET	r_o	0.368±0.004	0.25±0.01
		R_o nm	5.9±0.1	7.9±0.3
<i>b</i>	monomer-dimer equilibrium + intramolecular emFRET	r_o	0.373±0.005	0.32±0.05
		\bar{r}_d dimer	-0.093	0.034
		K_d mM	3.6±1.1	0.19±0.06
<i>c</i>	monomer-dimer equilibrium + intramolecular emFRET + intermolecular emFRET with monomer and dimer acceptors	r_o	0.373±0.006	0.41±0.11
		R_o nm	4.3	5.9±0.9
		K_d mM	2.5	0.034
		$\psi = r_{o,d} / r_{o,m}$	0.23	0.33±0.03

The fit designations correspond to panels *a*, *b*, *c* of Figure 4. Values without ± indications had fit errors of 50-100% differing between regressions with and without weighing factors. Quantities in italics are physically unrealizable. The value assumed for σ was 3/19 (Figure 1).

ACKNOWLEDGMENTS

T.M.J. was supported by the Max Planck Society, European Union FP5 Projects QLG1-2000-01260, QLG2-CT-2001-02278, QLK3-CT-2002-01997, and the Center of the Molecular Physiology of the Brain funded by the German Research Council (DFG). J.N.P. was supported by grant AR-246-2 to Donna Arndt-Jovin from the German Research Council (DFG). We indebted to Reinhard Klement, Bernd Rieger, and Keith Lidke for contributions to aspects of the analysis of the VFP crystallographic dimer, and to Donna Arndt-Jovin for critical reading of the manuscript. Venus VFP in pCS2+ was the kind gift of A. Miyawaki.

REFERENCES

1. V. Subramaniam, Q. S. Hanley, A. H. A. Clayton and T. M. Jovin, "Photophysics of green and red fluorescent proteins: some implications for quantitative microscopy," *Methods Enzymol.* **360**, 178-201, 2003.
2. A. H. A. Clayton, Q. S. Hanley, D. J. Arndt-Jovin, V. Subramaniam and T. M. Jovin, "Dynamic fluorescence anisotropy imaging microscopy in the frequency domain (rFLIM)," *Biophys. J.* **83**, 1631-1649, 2002.
3. D. S. Lidke, P. Nagy, B. G. Barisas, R. Heintzmann, J. N. Post, K. A. Lidke, A. H. A. Clayton, D. J. Arndt-Jovin and T. M. Jovin, "Imaging molecular interactions in cells by dynamic and static fluorescence anisotropy (rFLIM and emFRET)," *Biochem. Soc. Trans.* **31**, 1020-1027, 2003.
4. C. Buehler, C. Y. Dong, P. T. C. So, T. French and E. Gratton, "Time-resolved polarization imaging by pump-probe (stimulated emission) fluorescence microscopy," *Biophys. J.* **79**, 536-549, 2000.
5. I. Gautier, M. Tramier, C. Durieux, J. Coppey, R. B. Pansu, J. C. Nicolas, K. Kemnitz and M. Coppey-Moisan, "Homo-FRET microscopy in living cells to measure monomer-dimer transition of GFP-tagged proteins," *Biophys. J.* **80**, 3000-3008, 2001.
6. G. Marriott and I. Parker, Eds. *Biophotonics, Part A. Methods Enzymol.* **360**. San Diego, CA, Academic Press, 2003.
7. J. Siegel, K. Suhling, S. Leveque-Fort, S. E. D. Webb, D. M. Davis, D. Phillips, Y. Sabharwal and P. M. W. French, "Wide-field time-resolved fluorescence anisotropy imaging (TR-FAIM): Imaging the rotational mobility of a fluorophore," *Rev. Sci. Instrum.* **74**, 2003.
8. M. Tramier, T. Piolot, I. Gautier, V. Mignotte, J. Coppey, K. Kemnitz, C. Durieux and M. Coppey-Moisan, "Homo-FRET versus hetero-FRET to probe homodimers in living cells," *Methods Enzymol.* **360**, 580-597, 2003.
9. Y. Yan and G. Marriott, "Fluorescence resonance energy transfer imaging microscopy and fluorescence polarization imaging microscopy," *Methods Enzymol.* **360**, 561-580, 2003.
10. A. Squire, P. J. Verveer, O. Rocks and P. I. H. Bastiaens, "Red-edge anisotropy microscopy enables dynamic imaging of homo-FRET between green fluorescent proteins in cells," *J. Struct. Biol.* **145**, in press, 2003.
11. C. E. Bigelow, D. L. Conover and T. H. Foster, "Confocal fluorescence spectroscopy and anisotropy imaging system," *Opt. Lett.* **28**, 695-697, 2003.
12. A. Volkmer, V. Subramaniam, D. J. Birch and T. M. Jovin, "One- and two-photon excited fluorescence lifetimes and anisotropy decays of green fluorescent proteins," *Biophys. J.* **78**, 1589-1598, 2000.
13. E. Jares-Erijman and T. M. Jovin, "Determination of DNA helical handedness by fluorescence resonance energy transfer," *J. Mol. Biol.* **257**, 597-617, 1996.
14. E. A. Jares-Erijman and T. M. Jovin, "FRET imaging," *Nat. Biotechnol.* **21**, 1387-1395, 2003.
15. G. H. Fredrickson, "Concentration depolarization of fluorescence in the presence of molecular rotation," *J. Chem. Phys.* **88**, 5291-5299, 1988.

16. T. Nagai, K. Ibata, E. S. Park, M. Kubota, K. Mikoshiba and A. Miyawaki, "A variant of yellow fluorescent protein with fast and efficient maturation for cell-biological applications," *Nat. Biotechnol.* **20**, 87-90, 2002.
17. D. A. Zacharias, J. D. Violin, A. C. Newton and R. Y. Tsien, "Partitioning of lipid-modified monomeric GFPs into membrane microdomains of live cells," *Science* **296**, 913-916, 2002.
18. G. J. Palm, A. Zdanov, G. A. Gaitanaris, R. Stauber, G. N. Pavlakis and A. Wlodawer, "The structural basis for spectral variations in green fluorescent protein," *Nat. Struct. Biol.* **4**, 361-365, 1997.
19. F. I. Rossell and S. G. Boxer, "Polarized absorption spectra of green fluorescent protein single crystals: transition dipole moment directions," *Biochemistry* **42**, 177-183, 2003.
20. I. Z. Steinberg, "Long-range nonradiative transfer of electronic excitation energy in proteins and polypeptides," *Annu. Rev. Biochem.* **40**, 83-114, 1971.
21. A. A. Heikal, S. T. Hess and W. W. Webb, "Multiphoton molecular spectroscopy and excited state dynamics of enhanced green fluorescent protein," *Chem. Phys.* **274**, 37-55, 2001.
22. S. R. Adams, R. E. Campbell, L. A. Gross, B. R. Martin, G. K. Walkup, Y. Yao, J. Llopis and R. Y. Tsien, "New biarsenical ligands and tetracysteine motifs for protein labeling *in vitro* and *in vivo*: synthesis and biological applications," *J. Am. Chem. Soc.* **124**, 6063-6076, 2002.
23. J. N. Forkey, M. E. Quinlan, M. A. Shaw, J. E. T. Corrie and Y. E. Goldman, "Three-dimensional structural dynamics of myosin V by single-molecule fluorescence polarization," *Nature* **422**, 399-404, 2003.
24. H. Wallrabe, M. Elangovan, B. A., A. Periasamy and M. Barroso, "Confocal FRET microscopy to measure clustering of ligand-receptor complexes in endocytic membranes," *Biophys. J.* **85**, 559-571, 2003.
25. P. Sharma, R. Varma, R. C. Sarasij, Ira, K. Gousset, G. Krishnamoorthy, M. Rao and S. Mayor, "Nanoscale organization of multiple GPI-anchored proteins in living cell membranes," *Cell* **116**, 577-589, 2004.